Aus dem Institut für Physiologie
der Medizinischen Fakultät Charité – Universitätsmedizin Berlin

DISSERTATION

Development of a tool to probe the biomechanical properties of the endothelial surface layer

zur Erlangung des akademischen Grades
Doctor medicinae (Dr. med.)

vorgelegt der Medizinischen Fakultät
Charité – Universitätsmedizin Berlin

von

Alex Marki

aus Budapest

Datum der Promotion: 14.2.2014

Table of contents

1. *Abstract*

In German language

Einführung: In vorhergehenden Untersuchungen konnten wir zeigen, dass in isolierten Endothelzellen aus humanen Nabelschnurvenen (HUVEC) durch pulsatile Wandschubspannung bei unidirektionaler laminarer Strömung („atheroprotective flow profile“) die Expression von Konnexin40 und HAS2 induziert wird. Dagegen wird die Expression von TNFα sowie C6- und V1-Transient Rezeptor Potential (TRP) Ionkanälen bei relativ niedriger, oszillierender Wandschubspannung (atherogenes Strömungsprofil) induziert. Wir konnten auch zeigen, dass durch ein atherogenes Strömungsprofil die Synthese der wichtigsten Komponente der endothelialen Oberflächenschicht (ESL), der Hyaluronsäure (HA) unterdrückt wird. In Verbindung mit der umfangreichen Literatur über die Bedeutung des ESL für die Schubspannungsempfindlichkeit von Endothelzellen führen diese Ergebnisse zu der Vermutung, dass die ESL eine zentrale Rolle in einem proatherogenen *circulus vitiosus* spielen könnte: durch atherogene Strömungsbedingungen wird die HA-Synthese reduziert, dies führt zur Reduktion der ESL Dicke und der Schubspannungs-Empfindlichkeit des Endothels und damit zur weiterer Unterdrückung der Hyaluronsäureexpression. Um diese Hypothese testen zu können und die Rolle von Hyaluronsäure und Schubspannung für Veränderungen der ESL zu überprüfen, wurde eine Methode zur direkte Messung der Eigenschaften und Dicke der ESL von primären kultivierten Endothelzelle entwickelt.

Methoden: Die Dicke der ESL beträgt ca. 0.5-1 µm und erfordert damit Messverfahren unterhalb der Auflösungsgrenze des Lichtmikrokops. Dies wurde durch Bestimmung des Durchmessers von Beugungsringen fluoreszierender Nanopartikel außerhalb der Fokusebene erreicht. Zur off-line Auswertung entsprechender mikroskopischer Aufnahmen erfolgte mit einem eigenen Programm zum automatisierten Einzelpartikel-Tracking. Neben der Bestimmung der Position des jeweiliges Partikels in den drei Raumachsen war so zugleich die Messung der Viskosität des umgebenden Mediums möglich.

Ergebnisse und Zusammenfassung: Über einen vertikalen Bereich von 4,5 µm betrug die Validität für die Lokalisation einzelner Nanopartikel in der Senkrechten 16 nm bei einer Präzision von etwa 5 nm in der Vertikalen und 5 nm in der Horizontalen. In ersten Experimenten mit HUVECs, konnten wir einen Anstieg der Viskosität in Bereichen nahe der Zelloberfläche mit einer Schichtdicke von etwa 1000nm zeigen. Dieser Bereich könnte der endothelialen Oberflächenschicht entsprechen. Somit hat das entwickelte Verfahren das

Potential, die biophysikalischen Eigenschaften der ESL, besonders Viskosität und Dicke, zu untersuchen. Damit können die wandschubspannungs-bedingten frühen Effekte der endothelialen Dysfunktion, insbesondere die Bedeutung der ESL und der Hyaluronsäure, weiter untersucht werden.

In English language

Introduction: We have recently found in isolated human umbilical vein endothelial cells (HUVEC) that turbulent (atheroprone) vascular shear stress (VSS) down regulates endothelial connexin 40 and up regulates C6- and V1-type transient receptor potential (TRP) channels. However the mechanism for these atheroprone changes is poorly understood. We have shown that atheroprone VSS profile down regulates the synthesis of a major component of the endothelial surface layer (ESL), hyaluronan (HA). These findings together with the extensive amount of publications showing the importance of ESL in endothelial VSS sensation led us to speculate, that HA might be part of an atheroprone circulus vitiosus: in the absence of atheroprotective VSS, HA expression decreases. This leads to decrease of vascular VSS sensitivity followed by further reduction of HA expression. Thus we aimed at developing a tool to probe the properties and thickness of the surface layer of cultured HUVECs to allow investigation the role of HA for VSS related alterations of the ESL.

Methods: A defocus imaging based single particle tracking application was developed. It allows tracking the 3D position of fluorescent nanobeads with a precision beyond the diffraction resolution limit. Local viscosity can be assessed by quantifying the nanobeads' Brownian motion.

Results and conclusion: For a vertical range of 4.5 µm, the validity of vertical single particle tracking was 16 nm, with a precision of about 5 nm. In the horizontal plane precision was 5 nm. In first experiments with HUVEC we could show an increase of local viscosity in a region close to the cell surface with a thickness of about 1000 nm which may correspond to the ESL. Thus, the established approach has the potential to study biophysical properties of the ESL, including thickness and viscosity. This should allow to investigate the alteration of ESL beside different pathological conditions.

2. Introduction

2.1. Endothelial cells

Endothelial cells (ECs) pave the lumen of every blood vessel in the human body. These cells form the interface between the blood stream and the tissues and therefore these cells have a pivotal role in the regulation of tissue perfusion with blood (via vessel diameter adjustment), transport of all kind of material (water, nutrients, mediators, cells) through the vessel wall, new vessel formation and in blood coagulation.

The ECs with their basal surface are attached to the basal lamina of the vessel wall via integrin transmembrane proteins which assemble into focal adhesion sites. On their lateral surface the ECs form intercellular connections with each other. These lateral endothelial connections are important in regulating the paracellular solute exchange (via tight junctions) and in endothelial signal propagation along the vessel wall (via gap junctions). The luminal endothelial surface is covered with the endothelial surface layer (ESL) [1].

2.2. Shear stress sensitivity of endothelial cells

In a living organism the blood flow exerted vascular shear stress (VSS) constantly acts on the endothelial surface thereby influencing the endothelial proteome and secretome. After exposure to VSS isolated ECs slow down their proliferation and migration rate, reorganize their cytoskeleton, realign according to the flow direction and release different vasoactive mediators (e.g. nitric oxide, prostaglandins) in a VSS magnitude-dependent manner. Furthermore the central role of VSS was recognized in heart development, in angio- and vasculogenesis and in the development of atherosclerosis for what reason great deal of attention is devoted to the field of endothelial mechanotransduction.

Atherosclerosis (AS) is the main cause of today´s leading cardiovascular illnesses (e.g. myocardial infarct, stroke, a. renalis stenosis etc.) which results in organ failure due to stenosis of the organ´s feeding artery. Atherosclerosis is known to be a multifactorial disease, however out of the known factors the exposure to proatherogenic flow profile is presumably of higher importance; dissection studies early in the last century have shown, that AS develops at such vessel sites (mainly bifurcations), where the vessel wall is exposed to lower shear stress with flow reversal. To explain the molecular background of atherogenesis, lot of energy is invested into exploration of those endothelial elements which are suppressed or induced by proatherogenic flow profile [2].

Such elements are for instance the connexins (CX) or the transient receptor potential (TRP) channels. The CXs are the building blocks of the gap junctions, which are intercellular junctions allowing exchange of small particles (e.g. calcium) between two connected cells. ECs at atherosclerotic lesions were found to contain less CX40 and more CX43 compared to healthy vascular sites. The TRP channels belong to a group of cell membrane located kation channels with several mechanosensitive members. TRP channels are presumed to play role in atherogenesis via mediating local inflammation of the vessel wall. To study the effect of atheroprotective and proatherogenic flow profile on the expression of endothelial CXs and TRP channels, we have treated freshly isolated human umbilical vein endothelial cells (HUVEC) with the aforementioned two flow patterns in a custom-made cone-and-plate system. In this system different flow profiles were generated on HUVECs via rotating a cone attached with its tip the bottom of a Petri dish of confluent HUVEC. During these studies we have found, that an atheroprotective flow profile can induce the amount of CX40 in HUVECs on both the mRNA- and protein level. This induction was attenuated by inhibiting PI3K or Akt, a well-known pathway of endothelial mechanotransduction [3]. Also we have found that a proatherogenic flow profile can induce the expression of C6 and V1 type TRP channels in ECs which may increase the inflammatory responses of these cells [4]. The proatherogenic shift in CX and TRP channel expression and its accompanying proinflammatory effects (e.g. reduced endothelial nitric oxide production and increased adhesion molecule expression) might be preventable by better understanding of the mechanisms which are triggered by VSS.
In general the endothelial basal focal adhesion sites, lateral cell junctions, nucleus and the apical surface structures like mechanosensitive ion channels or the ESL are found to be responsible for endothelial mechanotransduction [2].

2.3. The endothelial surface layer

The ESL is a highly hydrophilic, 0.5-3.5 μm thick gel-like layer paving the entire vasculature. ESL involves a profound, approx. 100 nm thick, directly membrane bound layer called endothelial glycocalyx (EG) and a superficial, several 100 nm thick, sedimentary layer, which is presumed to be bound to the endothelial cell membrane indirectly via the EG ***(Fig.1.)***.

Detection of the ESL/EG thickness with regular brightfield or fluorescent microscopy is greatly limited. The refraction index of these structures is very similar to the one of blood plasma, thus brightfield microscopy with contrast enhancement can´t make it visible. The layer can be stained for its sugar or protein components, however the measurement of its thickness is greatly hindered by the diffraction limit of resolution inherent in every conventional light or fluorescent microscope. The theory behind that was published for the first time by Ernst Karl Abbe German physicist in 1873, according to that the diffraction limit of resolution is provided by the wave nature of light and it depends on the wavelength of the detected light. The diffraction limit of resolution can be calculated as $0.61\lambda/NA$ in lateral and $\lambda \cdot n/NA^2$ in axial direction, respectively, where λ is the recorded wavelength, n is the refractive index of the propagation medium, and NA is the numerical aperture of the imaging system. *(Accordingly our optical setup (λ = 560 nm, NA = 1.3 and n = 1.45) is limited by ~ 260 nm lateral, and ~ 450 nm axial resolution.)* To overcome the diffraction limit of resolution several fluorescence microscopic techniques have been employed (e.g. STED with lateral resolution ~ 20 nm or TIRF with axial resolution < 100 nm), but these complex and expensive techniques are not applicable for the thickness measurement of the ESL because either they operate on horizontal plane (like STED) or their vertical working distance is to short (e.g. for TIRF it is limited to about 800 nm). Electron microscopy offers a fundamental solution to the diffraction limit via detecting electron beam which has about 100.000 times shorter wavelength compared to light beam. However electron microscopy requires harsh fixation of the sample.

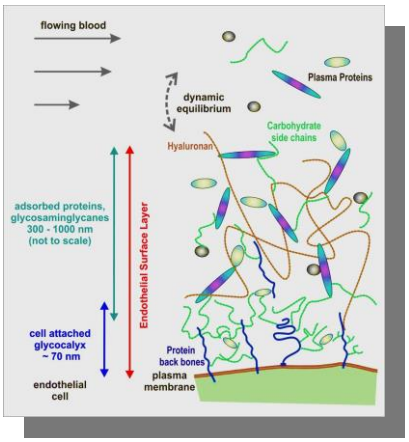

Figure 1. Schematic representation of the endothelial surface layer; a superfitial sedimentary layer is presumambly bound to the endothelial cell via the directly membrane bound endothelial glycocalyx. Modified from [5] .

With electron microscopy (after labeling the carbohydrates with lanthanum nitrate or Alcian blue staining) the maximal EG thickness was found to be about 100 nm in cardiac capillaries, which is in accordance with the known length of the EG core proteins. However intravital microhemodynamical studies conducted in arteriolaes and capillaries predicted a much thicker surface layer.

In vivo enzymatic degradation of the ESL with heparinase or hyaluronidase treatment was found to elevate the tube hematocrit as a measure for the increased effective diameter in

cremaster arterioles or skin micro-vessels. The flow resistance in cremaster micro-vessels was found to be higher compared to glass capillaries of the same apparent diameter, suggesting the presence of a surface layer thicker than 100 nm. These findings were corroborated by the tracer dilution technique, where the diameter of the lumen occupied by fluorescently labeled dextran molecules was compared to the internal diameter of the vessel visible with bright-field microscopy. The difference between the diameters measured in the two ways assumes the presence of a 400-500 nm thick endothelial surface layer. Further evidence for the presence of an about 500 nm thick ESL in micro-vessels was provided with the help of a micro-particle image velocimetry (μ-PIV) based flow profile reconstruction. For this the convective displacement and radial position of fluorescent tracer particles flown trough a micro-vessel were determined along a time lapse record. The extrapolation of the reconstructed flow profile revealed complete stasis of flow already 500 nm away from the apparent vessel wall.

The difference between the surface layer thickness obtained with electron microscopy or with the mentioned techniques is explained with the gross sensitivity of the absorbed part of the layer toward fixation for electron microscopy.

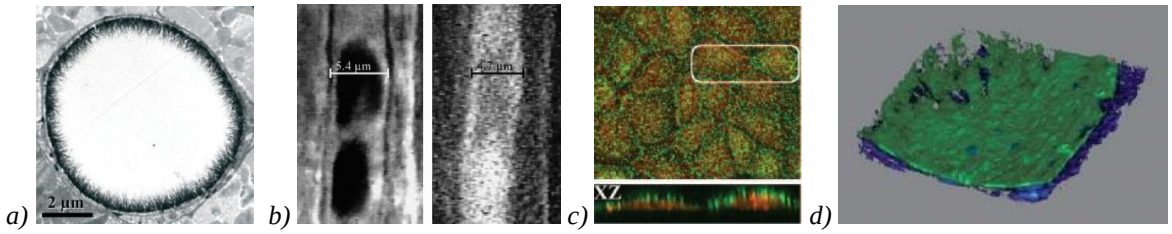

Figure 2. Examples of EG and ESL imaging: a) electron micrograph with Alcian blue staining of EG in a cardiac capillary, b) tracer exclusion technique shows that the ESL of a mesentery capillary can exclude from itself fluorescent tracer particles, c) confocal scanning microscopy image of fixed endothelial cells stained with anti heparan sulphate antibody (green) and cell tracker (orange), d) two photon scanning miroscopy image of the endothelial surface of an isolated vessel stained with specific sugar moiety binding lectin (green) and a cell tracker (blue). For the original articles please see [6,7,8].

The ESL is made up by components originating either from blood or endothelial cells, which are proteoglycans (vastly with heparin sulphate side chains), hyaluronan (HA), glycoproteins (e.g. selectins), proteins (mainly serum albumin), ions and water. Proteoglycans are the most represented components of the ESL, furthermore the proteoglycans via their negative charge and the ESL bound albumin via generating higher osmotic pressure are responsible for keeping the layer hydrated. The higher osmotic pressure together with the mechanical

stiffness of the scaffold elements (proteoglycans and hyluronan) is hypothesized to maintain the thickness of the ESL.

The ESL is presumed to regulate microhemodynamics via influencing the tube hematocrit and the flow induced vasodilatation (through mediating shear stress sensation). Also ESL is suggested to have a role in inflammatory processes; inflammatory mediator TNFα was shown to induce ESL shedding and according to some evidence the ESL can regulate leukocyte arrest via shielding the endothelial – leukocyte adhesion molecules from each other. Furthermore via its permeability barrier role, the ESL was found to be important in regulating solute exchange across the vessel wall e.g. in the kidney. For this section please find the original articles in the reviews [5,6].

2.4. Role of the endothelial surface layer in shear stress sensation

Large amount of evidence supports the hypothesis, that ESL (or EG) contributes to endothelial shear stress sensation. Treatment of the endothelial surface with GAG digestive enzymes (heparinase, hyaluronidase or neurmaminidase) was found to attenuate several flow induced endothelial response in cultured endothelial cells (cytoskeleton remodeling and cell realignment, nitric oxide synthesis) in isolated and perfused vessels (flow induced vasodilation) in Langendorf-heart model (coronary dilation) and *in vivo* vessel preparations (reactive hyperemia and flow induced vasodilation). Furthermore modeling studies have found that ESL shields completely the EC membrane from VSS. The role of ESL in endothelial mechanotransduction was greatly reviewed by Tarbell and Pahakis [9].

Based on this considerations ESL is presumed to transmit the VSS into the endothelial cells via its transmembrane core proteins, which are mainly the heparin-decorated syndecans. This matches well with the finding, that exposure to heparinase can attenuate endothelial mechanotransduction, however it does not explain, why degradation of the non transmembrane, CD44-anchored hyaluronan (HA) has a similar effect. An explanation could be, that the 2-25 μm 10^3-10^4 kDa large macro molecule HA has an ESL cross-linking function, which helps to maintain the intact structure of the ESL.

To gain further insight into the presumed role of HA in endothelial mechanotransduction, we tested the effect of different shear stress profiles on the expression level of HA synthase 2 and of HA in cultured HUVECs. We have found that an atheroprotective flow profile induced HA synthase 2 on both mRNA- and protein level and significantly increased the amount of surface bound and secreted HA [10]. Our results match well with the observation that the ESL

is found to be reduced at atheropredilected vessel sites with their typically distributed flow conditions [7].

If HA indeed functions like a bond keeping together the ESL, a circulus vitiosus (self accelerating pathomechanism) could be envisaged; upon the development of proatherogenic flow profile and thus loss of healthy stimulus, endothelial shear stress sensing is further reduced via reduction of HA synthesis and diminishment of the presumed shear stress sensor ESL ***(Fig.3.)***.

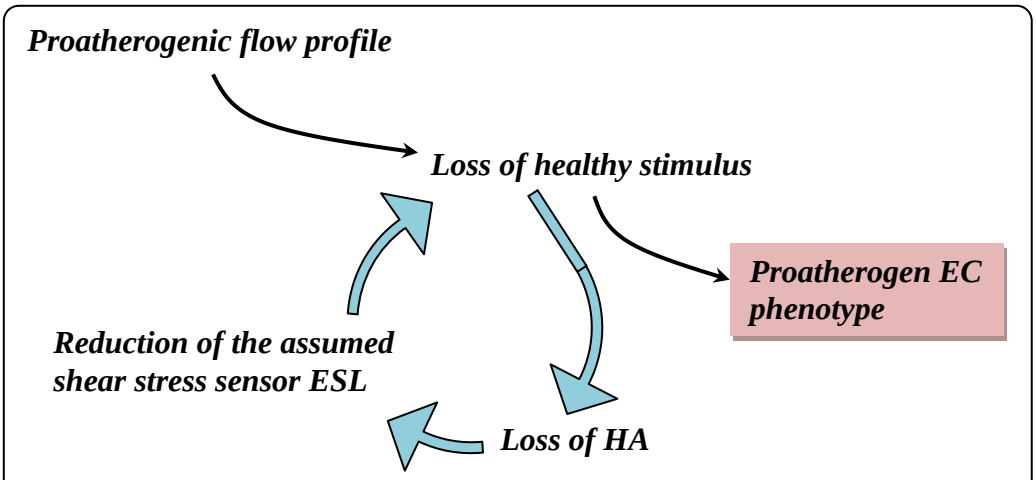

Fig.3. Scheme of hypothesized self-amplifying pathomechanism in atherosclerosis development. For explanation see the text.

Therefore to further investigate the hypothesized effect of HA in maintaining the ESL structure, we aimed to set up an assay to probe the biomechanical properties of the ESL.

2.5. Objective

The objective of this work was to develop a novel tool to study *in vitro* in living cells and later *in vivo* in living organisms the biomechanical properties (thickness, density and resistance) of the endothelial surface layer. We propose to track with high precision the motion of different fluorescent nanobeads situated in the close vicinity of the endothelial surface. While without the presence of convective flow the nanobeads´ trajectories are dominated by their thermal vibration i.e. Brownian motion (BM), in the presence of convective flow the nanobeads´ trajectories show a vast unidirectional component. It was already shown that ESL can attenuate the flow of fluorescent tracer particles and thus the flow of blood serum in the 500 nm vicinity of the vessel wall [11]. However based on the Stokes-Einstein law, which says that BM of particles embedded in a medium show an inverse relationship to the viscosity of

the embedding medium, it is reasonable to expect that ESL via increasing the local viscosity should reduce the BM of those fluorescent particles which invade the ESL. Due to this, quantification of the BM of the particles situated in the few hundred nanometer vicinity of the endothelial cell membrane should report about the ESL´s viscosity.

The proposed approach requires 3D single particle tracking (SPT) to detect the horizontal coordinates of the particle which provide readout of the local viscosity and the vertical coordinate of the particle which provides the distance from the endothelial cell membrane. To enable punctual viscosity measurement from BM trajectories reconstructed from high frame rate records and to resolve the few hundred nanometer vertical distance from the endothelial cell membrane, the SPT should function with precision beyond the diffraction limit of resolution.

For this purpose centroid determination in combination with defocus imaging technique offers a practical and budget friendly solution, where real time localization of tracer particles on living cell is enabled via calculating the center of the spherical tracer particle´s image and via decoding precisely the particle – focal plane distance from the particle´s defocus image. The defocus imaging technique utilizes the strong relationship between a light source´s distance from the focal plane and its corresponding defocus image; a light source situated exactly in the focal plane will appear as a more or less sharp spot but as the light source gets further away from the focus plane, its image turns into a gradually growing diffraction image ***(Fig.3)***.

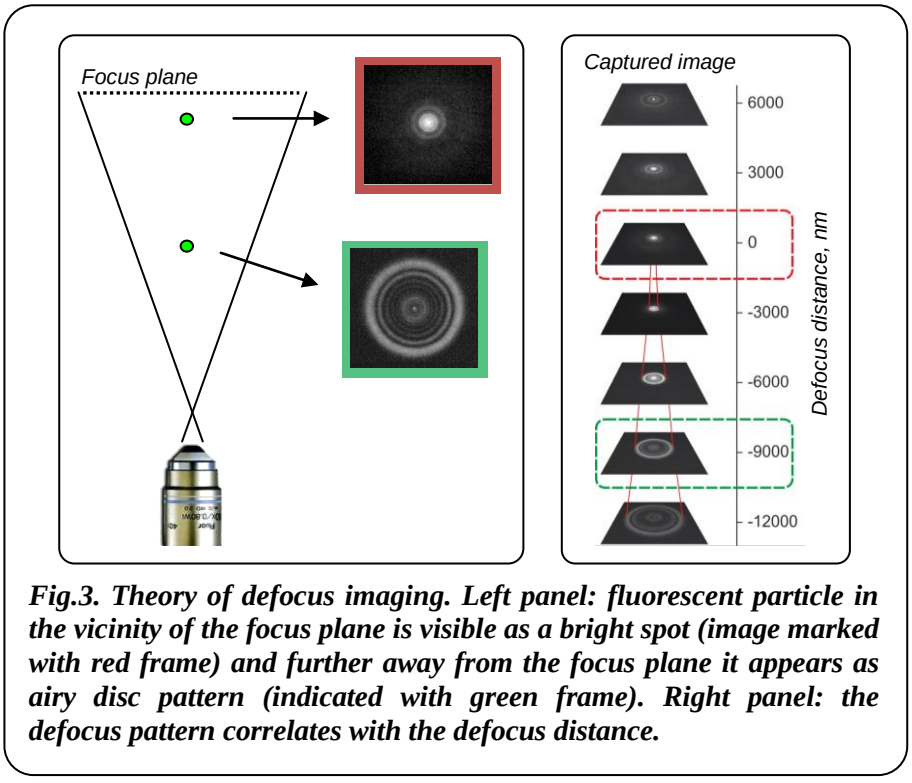

Fig.3. Theory of defocus imaging. Left panel: fluorescent particle in the vicinity of the focus plane is visible as a bright spot (image marked with red frame) and further away from the focus plane it appears as airy disc pattern (indicated with green frame). Right panel: the defocus pattern correlates with the defocus distance.

These imaging techniques do not increase the spatial resolution of an optical system, but allow horizontal and vertical localization of a fluorescent particle with a precision beyond the resolution limit.

Thus to establish the proposed ESL probing tool we aimed to develop a centroid calculation and defocus imaging three-dimensional single particle tracking application.

3. Methods

3.1. Optical setup

An inverted microscope (Diaphot DMT, Nikon, Japan) equipped with a 100 W mercury arc lamp, with a piezo objective positioner (PI, Germany), a Plan-Neofluar 100x/1.3 Oil objective (Zeiss, Germany) and a CCD digital camera (DX4, Kappa Opto-electronics, Germany) was used. The camera and the objective positioner were controlled with a personal computer *via* an interface device (RedLab 3105, Meilhaus Electronic, Germany). The pattern of image capture and objective movement by the piezo positioner were programmed in interface software (ProfiLab Expert 4.0).

Polystyrene particles (FluoSpheres, Molecular Probes, Oregon) with 200 ± 40 nm diameter and carboxylated – negatively charged coating were used. These nanobeads had an excitation peak of λ_{ex} = 540 nm and an emission peak of λ_{em} = 560 nm.

3.2. Single particle tracking

To perform the high precision vertical tracking ***(Fig.3)***, firstly calibration images were obtained of a nanobead beside known nanobead – focus plane (i.e. defocus) distances. For this a vertical image stack of a nanobead entrapped in a distilled water film-layer between an ordinary microscopy slide and cover slip was prepared (10,000 nm wide defocus range with 50 nm steps) using a piezo objective positioner. The obtained images were annotated with the set relative defocus distance. Next, the image of a nanobead of interest was compared to the previously obtained calibration images. The defocus position of the analyzed nanobead was provided by the most similar reference image. To overcome the resolution limit provided by the 50 nm step size of the calibration stack, the two most fitting images of the stack were linearly increased or decreased until they showed the strongest correlation to the analyzed pattern. With the received scale factor the precision of the vertical tracking was pushed beyond the step-size resolution of the reference vertical image stack. The analyzed image was

compared to the calibration images with a custom-made software via Fourier transformation analysis. The horizontal position determination (i.e. the centroid determination) happened in the same image comparison step used to find the vertical position via fitting the most correlating 2D Fourier transformation image to a 2D parabola. The peak position of this parabola determined the x-y position of the particle with sub-pixel resolution.

To assess the validity of vertical position tracking, nanobeads were tracked trough a vertical image stacks, and the standard deviation (SD) of the decoded defocus distances from their fit line was taken. To characterize the vertical tracking precision, more than 100 defocus images were taken of nanobeads meanwhile the focus plane was displaced with a rectangular (50 nm) wave on a slope pattern. Vertical positions of two nanobeads were tracked along the images and the vertical distance between the two nanobeads was calculated for every image. The SD of the distance values was taken to characterize the precision. The lateral tracking precision was tested in the same analogy; horizontal distance between two nanobeads was calculated along a record where the sample was displaced with a 50 nm large rectangular wave pattern.

3.3. Measurement of medium viscosity and reconstruction of near-wall flow profile

Nanobeads were dispersed in a lower viscosity (phosphate salt buffer, PBS) or in a higher viscosity (PBS+Dextran 150 kDa). The viscosity of PBS and PBS+Dextran solutions was repeatedly measured at 37°C with a capillary viscometer (Ubbelohde-viscometer, Schott, Germany). The media with the nanobeads were loaded into a cell free micro flow-chamber (μ-slide I Luer, IBIDI, Germany) of which the bottom was marked with adhered nanobeads. Nanobead trajectories were recorded (for 6 sec with 3 FPS frame rate) in the absence or presence of convective flow generated by a perfusion pump (Braun, Germany), frame-to-frame displacements of the nanobeads were tracked.

For viscosity measurement via BM quantification the record in the absence of convective flow was used. The BM of the nanobeads was quantified via mean square displacement (MSD) calculations:

$$\mathrm{MSD} = 2Dt = \frac{1}{n}\sum_{i=0}^{n}(s^2{}_i)$$

where D is the diffusivity of the nanobead in the given medium, t the time delay between two capture of two captured positions, s the displacement in x or y or z direction, and n is the number of analysed images. According to the Stokes Einstein law, D is inversely proportional to the viscosity of the medium, which means that MSD is inversely proportional with the

viscosity. As a consequence, the ratio between MSD values measured for nanobeads solved in media with high and low viscosity must be equal to the inverse ratio of media viscosities. In precision assessment of MSD calculation (i.e. BM quantification) trajectories of 8 particles (all together 136 steps) were analysed for each medium.

The near-wall flow profile was reconstructed via PIV and its result i.e. the relation between a nanobead´s convective displacement and its radial position was compared to the predictions based on flow volume measurements (from the measured volume flow the mean flow velocity was calculated with the help of the dimensions of the flow chamber, via estimating the maximal flow velocity as 1.5 times the mean flow velocity a parabolic vertical flow profile was plotted).

3.4. Cell culturing

Human umbilical vein endothelial cells (HUVEC) were isolated and cultivated in a standard cell culture flask with a specific endothelial medium (from PromoCell-Germany, supplemented with 5% fetal calf serum, endothelial cell growth supplement, epidermial growth factor, hydrocortisone, heparin, 0,5% penicillin streptomycin). The confluent HUVECs were detached with trypsin and then seeded into a flow chamber. After confluence, some of the HUVEC samples were incubated with 100 U/mL TNFα (Peprotech, USA) for 4hours to induce shedding of the ESL. The other part of the sample was kept as non-treated controls. Afterwards the cell samples were further incubated on the stage of the microscope with the help of an on-stage incubator (Ibidi, Germany) which maintained 5% CO_2, 37°C and humidity around the sample. After half an hour equilibration time the nanobeads dispersed in culturing medium were applied on the cells, and in the absence of convective flow for half an hour every 10 minutes in 5 μm vicinity of the endothelial cell membrane the motion of nanobeads was recorded with a framing rate of 50 FPS with the above described optical system.

4. *Results*

4.1. Validity and precision of single particle tacking

Raw data of the vertical image stack analysis are shown on ***Fig.4,A***, where the defocus distance values set by piezo positioner are plotted against the calculated defocus distance values. Vertical position determinations functioned with about 40 nm and 16 nm validity on long (from 3000 to 10000 nm) and on short (from 5000 to 9500 nm) defocus ranges, on the plot the vertical dotted lines show the upper and lower boarder of the short defocus range.

On ***Fig.4,B*** the calculated Δ defocus positions of a nanobead during 50 nm wave on a slope focus plane displacement maneuver are shown in the dependence of time. The precision of vertical tracking was calculated to be 5 nm (variable coefficient 4.6%).

On ***Fig.4,C*** a nanobead´s calculated Δ y-axis position during the lateral rectangular wave displacement is shown. During this test the lateral position tracking functioned with 7 nm precision (variable coefficient 0.02%). Due to lack of lateral sample positioner with certified validity and precision, the validity of lateral tracking was not assessed.

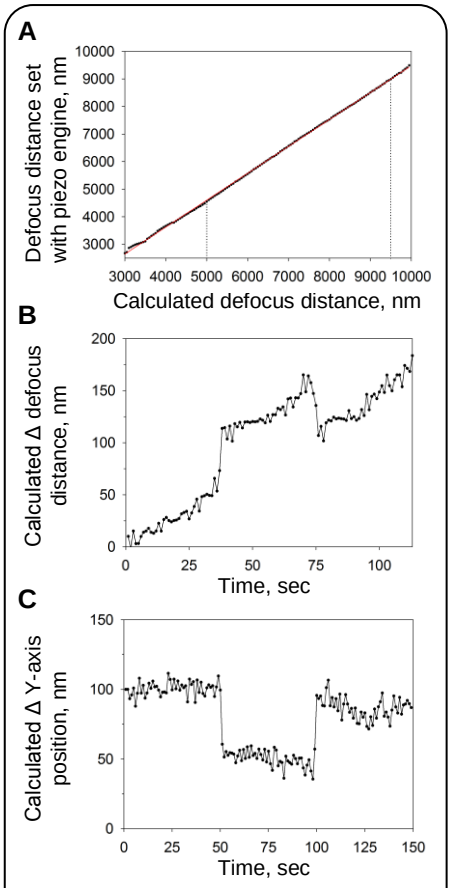

Fig.4. Performance test of the single particle tracking method. A – validity of vertical position tracking, B and C precision of vertical and lateral position tracking. For explanation see the text.

Underexposure of nanobeads had only a slight effect on the vertical tracking performance (vertical precision: underexposed 32 nm vs. optimally-exposed 16 nm). Distortion of patterns of endocytosed nanobeads or overlap of patterns of nanobeads close to each other significantly reduced the tracking performance but the precision still stayed beyond the resolution limit (vertical precision: distorted pattern 17 nm and overlapping pattern 42 nm vs. control 5 nm).

4.2. Viscosity measurement and near-wall flow profile reconstruction

Viscosity measurement with capillary viscometer yielded 0.7cP for PBS and 6.2cP for PBS+Dextran solution, from which values 8.8 viscosity ratio was calculated for the two solutions.

In accordance with theory, nanobeads showed reduced BM in PBS+Dextran medium with higher viscosity, than in PBS medium with lower viscosity ***(Fig.6.)***. The BM quantification via MSD calculation along x-, y- and z-axis functioned with precision of 11.8±1 % and 13±3 % for nanobeads embedded in lower and higher viscosity medium, respectively. For each axis the ratio between low and high viscosity MSD was in reciprocal correlation with the ratio between the low and high viscosity values of the respective medium (MSD_{PBS} / $MSD_{PBS+DEX}$ = 8.4 (x) and 8.8 (y) and 8.9 (z) vs. $visc._{PBS+DEX}$ / $visc._{PBS}$ = 8.8).

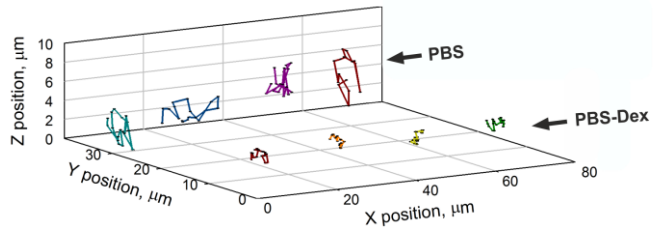

Fig.6. 3D trajectories of nanobeads showing Brownian motion in low viscosity PBS and in high viscosity PBS+Dextran media.

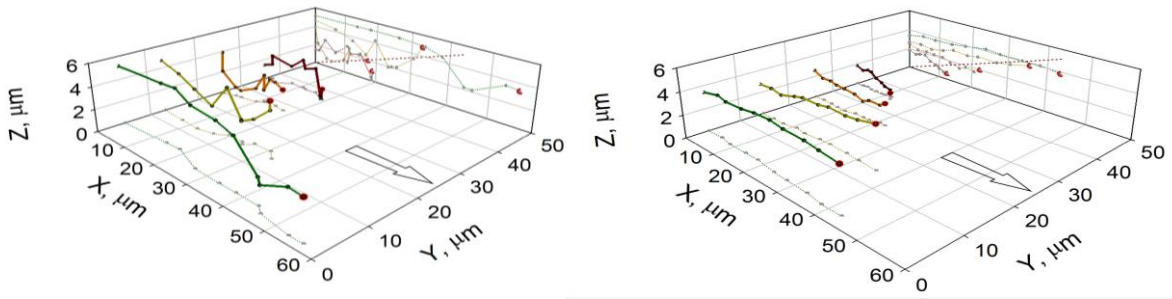

Fig.7. Near-wall flow profile tracking beside different viscosity media. For better visibility the nanobead trajectories were rearranged along the horizontal plane.

In the presence of convective flow the trajectories of nanobeads embedded in PBS and PBS+Dextran were successfully reconstructed from the coordinates obtained via performing frame-to-frame SPT along the record ***(Fig.7.)***. The trajectories were reconstructed in 4 µm vicinity of the bottom surface. It is clearly visible that higher medium viscosity reduced the nanobeads´ deviation from their convective displacement and thus the distance the nanobeads travelled during the acquisition time matched better with the one predicted from the flow volume measurement (the red dotted line on the xz-plane indicates the values predicted from the volume flow measurement).

4.3. Probing the endothelial surface layer

In a nearly 1-µm thick layer adjacent to the cell membrane surface 2.5 times higher viscosity was measured compared to that obtained more remote from the cell membrane. After preincubation of the cells with TNF-α, this layer was found to be greatly reduced and only a

remnant with a maximal relative viscosity of 1.5 close to the cell membrane was observed ***(Fig.7.)***.

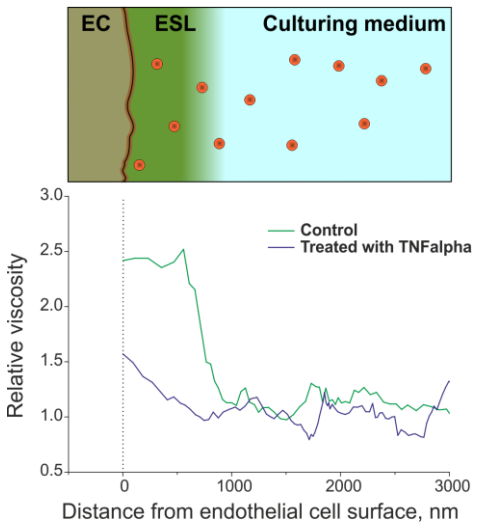

Fig.7.Probing the viscosity near the endothelial cell membrane

5. Discussion

The developed three dimensional single particle tool functions with 16 nm validity and 5 nm precision along the vertical plane and 5 nm precision along the lateral plane, which values are far beyond the diffraction resolution limit of light microscopy. The tool enables viscosity measurement and flow profile reconstruction in the close vicinity of a cell surface and thereby it enables much more precise estimation of thickness and biomechanical properties of the ESL of cultured cells or blood vessels. This could be used to investigate all those mechanisms which determine ESL thickness and function.

The present study proposes an ESL probing approach based on the assumption that fluorescent nanobeads can invade the ESL and that their Brownian motion or their displacement with the convective flow will be hampered by the mechanical resistance of the ESL. To track the vertical position of the nanobeads a tool was developed, which derives the nanobeads´ defocus distance from the whole pattern of their defocus image. The defocus distance is linearly related to the diameter of the defocus image thus after determination of the equation which describes the relationship between the defocus distance and the diameter of the defocus image, solely the diameter of the whole pattern can be used as well for vertical position tracking. Although this approach has inherently unlimited resolution, it utilizes only a little information of the defocus image and therefore it is more sensitive to underexposure or optical distortion of the defocus image then the approach where the whole pattern is used to decode the defocus distance. In the latter the defocus distance is derived via comparing the whole defocus image to the 3D point spread function (PSF) of the detected particle. The PSF of a light source is dependent on the diffraction characteristics of the used microscope elements (e.g. objective, coverslip, immersion medium, etc.) and it can be determined via modeling calculations. While modeling offers a continuous PSF, it is only approximating the real PSF because the modeling utilizes the nominal characteristics of the optical setup which usually differ to some extent from the real ones. To overcome this problem the present method utilizes an empirically established PSF which is reconstructed from a recorded

vertical image stack. This PSF reflects the true optical situation, but its resolution is limited to the step size of vertical image stack. To ´cover´ the gaps between the steps, selected images of the vertical stack are linearly increased or decreased with an image processing algorithm.

Crucial part of the proposed ESL probing method is the type of tracer particle chosen for measurement. The particle´s size, charge and coating will influence the interaction between the particle and the probed environment (e.g. blood serum, cytosol or ESL). The tracer dilution experiments have shown that negatively charged dextrans larger than 40kDa (Stokes radius about 5 nm) can´t invade the layer within three hours of incubation. On the other hand according to a recent report, negatively charged gold nanoparticles with 137 nm diameter could invade within hours the surface layer of different cancer cell lines [12]. This discrepancy could be explained with the difference between the composition of the surface layer of an endothelial and of a tumour cell. Apart from the charge, it is important to choose probing beads with appropriate size. Too small size of the particle greatly hampers its detection, and may require powerful illumination which is known to be detrimental for the ESL. Conjugation of albumin to a fluorescent particle was found to increase the diffusion rate of the particle, what suggests the importance of the molecular structure of the particle in its diffusion trough the ESL.

The technique proposed in the present study has two major benefits; the tracking of point-like fluorescent tracers allows the application of such single particle tracking algorithms (defocus imaging for vertical and centroid calculation for horizontal localization) which bring the tracking precision beyond the diffraction limit of resolution. Second, the approach is very sensitive, because the readout of signal is the BM. Fan et al have recently demonstrated the sensitivity of a BM based assay via detecting antigen in a solution with the help of antibody coated nanoparticles. When the antigens bound to the nanoparticles due to their increased diameter the nanoparticles showed a reduced BM [13]. To leverage the inherent sensitivity of the proposed BM approach, extra care has to be taken to isolate the measurement from external noises which could lead to vibration and from temperature fluctuations which could affect the intensity of BM.

The mechanical resistance of the ESL can be measured with atomic force microscopy, for that the cantilever of the device has to be equipped with a micro bead to provide a larger surface to intend the ESL [14]. This is a very straightforward technique, but it has a limited sensitivity, it is applicable only *in vitro* and it requires a very special technical background. Recently ESL resistance was estimated from the finite fluctuation movement of glass microspheres applied on the top of cultured endothelial cells. The fluctuation was assumed to be dependent on the

ESL stiffness and it was detected with reflectance interference contrast microscopy ®™. The interpretation of ESL stiffness with this interesting approach is difficult. The density or porosity of the layer was studied via measuring the time necessary for different fluorescently labeled molecules to invade the ESL [15]. As a demonstration of the proposed ESL probing concept, on ***Fig,7.*** a preliminary data of ESL viscosity measurement is shown. During this experiment one HUVEC sample was incubated with TNFα, which is an inflammatory mediator known to induce shedding of the ESL, and another HUVEC sample was kept as control. After about half hour incubation with nanobeads applied onto the cells, in case of the TNFα treated group the nanobeads situated closer to the cells showed reduced BM. This observation could be interpreted in the way, that the ESL shed by the TNFα treatment became more permeable toward the nanobeads.

The introduced technique via its potential to provide precise measurements of the ESL´s biomechanical characteristics may foster our better understanding of vessel wall permeability, regulation of microrheology and circulating cell extravasation which processes all have a clinical relevance.

6. List of abbreviations

BM	Brownian motion	**PIV**	Particle image velocymetry
CX	Connexin	**PSF**	Point spread function
EC	Endothelial cell	**SD**	Standard deviation
EG	Endothelial glycocalyx	**SPT**	Single particle tracking
ESL	Endothelial surface layer	**TRP**	Transient receptor potential (channel)
GAG	Glycosaminoglycan	**VSS**	Vascular shear stress
HA	Hyaluronan		

7. List of references

1. Pries, A.R. and W.M. Kuebler, *Normal endothelium.* Handb Exp Pharmacol, 2006(176 Pt 1): p. 1-40.
2. Davies, P.F., *Hemodynamic shear stress and the endothelium in cardiovascular pathophysiology.* Nat Clin Pract Cardiovasc Med, 2009. **6**(1): p. 16-26.

3. Vorderwulbecke, B.J., et al., *Regulation of endothelial connexin40 expression by shear stress.* Am J Physiol Heart Circ Physiol, 2012. **302**(1): p. H143-52.

4. Thilo, F., et al., *Pulsatile atheroprone shear stress affects the expression of transient receptor potential channels in human endothelial cells.* Hypertension, 2012. **59**(6): p. 1232-40.

5. Pries, A.R., T.W. Secomb, and P. Gaehtgens, *The endothelial surface layer.* Pflugers Arch, 2000. **440**(5): p. 653-66.

6. Reitsma, S., et al., *The endothelial glycocalyx: composition, functions, and visualization.* Pflugers Arch, 2007. **454**(3): p. 345-59.

7. VanTeeffelen, J.W., et al., *Endothelial Glycocalyx: Sweet Shield of Blood Vessels.* Trends Cardiovasc Med, 2007. **17**(1): p. 101–105.

8. Thi, M.M., et al., *The role of the glycocalyx in reorganization of the actin cytoskeleton under fluid shear stress: a "bumper-car" model.* Proc Natl Acad Sci U S A, 2004. **101**(47): p. 16483-8.

9. Tarbell, J.M. and M.Y. Pahakis, *Mechanotransduction and the glycocalyx.* J Intern Med, 2006. **259**(4): p. 339-50.

10. Maroski, J., et al., *Shear stress increases endothelial hyaluronan synthase 2 and hyaluronan synthesis especially in regard to an atheroprotective flow profile.* Exp Physiol, 2012. **96**(9): p. 977–986.

11. Smith, M.L., et al., *Near-wall micro-PIV reveals a hydrodynamically relevant endothelial surface layer in venules in vivo.* Biophys J, 2003. **85**(1): p. 637-45.

12. Zhou, R., et al., *Slowed diffusion of single nanoparticles in the extracellular microenvironment of living cells revealed by darkfield microscopy.* Anal Bioanal Chem, 2011. **399**(1): p. 353-9.

13. Fan, Y.J., et al., *A quantitative immunosensing technique based on the measurement of nanobeads' Brownian motion.* Biosens Bioelectron, 2009. **25**(4): p. 688-94.

14. Oberleithner, H., et al., *Salt overload damages the glycocalyx sodium barrier of vascular endothelium.* Pflugers Arch, 2011. **462**(4): p. 519-28.

15. Job, K.M., R.O. Dull, and V. Hlady, *Use of reflectance interference contrast microscopy to characterize the endothelial glycocalyx stiffness.* Am J Physiol Lung Cell Mol Physiol, 2012. **302**(12): p. L1242-9.

Affidavit

I, Alex Marki certify under penalty of perjury by my own signature that I have submitted the thesis on the topic “Development of a tool to probe the biomechanical properties of the endothelial glycocalyx” I wrote this thesis independently and without assistance from third parties, I used no other aids than the listed sources and resources.

All points based literally or in spirit on publications or presentations of other authors are, as such, in proper citations (see "uniform requirements for manuscripts (URM)" the ICMJE www.icmje.org) indicated. The sections on methodology (in particular practical work, laboratory requirements, statistical processing) and results (in particular images, graphics and tables) correspond to the URM (s.o) and are answered by me. My contributions in the selected publications for this dissertation correspond to those that are specified in the following joint declaration with the responsible person and supervisor. All publications resulting from this thesis and which I am author of correspond to the URM (see above) and I am solely responsible.

The importance of this affidavit and the criminal consequences of a false affidavit (section 156,161 of the Criminal Code) are known to me and I understand the rights and responsibilities stated therein.

Date Signature

Declaration of any eventual publications

Alex Marki had the following share in the following publications:

Publication 1:
Alex Marki, Eugeny Emilov, Andreas Zakrzewicz, Akos Koller, Timothy W. Secomb, Axel R. Pries; *Tracking of fluorescence nanoparticles with nanometre resolution in a biological system: assessing local viscosity and microrheology*; Journal of Biomechanics and Modelling Mechanobiology; 2013.
Alex Marki has taken part in: the planning of the project, obtaining and analysing the data, writing the text and preparing the figures.

Publication 2:
Florian Thilo, Bernd J. Vorderwülbecke, **Alex Marki**, Katharina Krueger, Ying Liu, Daniel Baumunk, Andreas Zakrzewicz, Martin Tepel; *Pulsatile atheroprone shear stress affects the expression of transient receptor potential channels in human endothelial cells*; Hypertension; 2012.
Alex Marki has prepared the endothelial cell samples for mRNA and Western blot analysis and he has participated in preparing the text.

Publication 3:
Bernd J. Vorderwülbecke, Julian Maroski, Katarzyna Fiedorowicz, Luis Da Silva-Azevedo, **Alex Marki**, Axel R. Pries and Andreas Zakrzewicz; *Regulation of endothelial connexin40 expression by shear stress*; Am J Physiol Heart Circ Physio; 2012.

Alex Marki has contributed to this work via obtaining Rt-qPCR data for it from endothelial cells, and via contributing to the manuscript preparation.

Publication 4:

Julian Maroski, Bernd J. Vorderwülbecke, Katarzyna Fiedorowicz, Luis Da Silva-Azevedo, Günter Siegel, **Alex Marki**, Axel Radlach Pries, Andreas Zakrzewicz; *Shear stress increases endothelial hyaluronan synthase 2 and hyaluronan synthesis especially in regard to an atheroprotective flow profile*; Experimental Physiology; 2012.

Alex Marki has contributed to this work with isolating and culturing human umbilical vein endothelial cells and with helping the preparation of the manuscript.

Signature, date and stamp of the supervising University teacher

_____

Signature of the doctoral candidate

Publications selected for publication promotion

1) **Marki A**, Ermilov E, Zakrzewicz A, Koller A, Secomb TW, Pries AR; Tracking of fluorescence nanoparticles with nanometre resolution in a biological system: assessing local viscosity and microrheology. *Biomech Model Mechanobiol. Date of publication: 11 June 2013.*

Impact factor: 3.19

2) Thilo F, Vorderwülbecke BJ, **Marki A**, Krueger K, Liu Y, Baumunk D, Zakrzewicz A, Tepel M; Pulsatile atheroprone shear stress affects the expression of transient receptor potential channels in human endothelial cells. *Hypertension. Date of publication: 7 May 2012.*

Impact factor: 6.2

3) Vorderwülbecke BJ, Maroski J, Fiedorowicz K, Da Silva-Azevedo L, **Marki A**, Pries AR, Zakrzewicz A; Regulation of endothelial Connexin-40 expression by shear stress. *Am J Physiol Heart Circ Physiol. Date of publication: 21 October 2011.*

Impact factor: 3.7

4) Maroski J, Vorderwülbecke BJ, Fiedorowicz K, Da Silva-Azevedo L, Siegel G, **Marki A**, Pries AR, Zakrzewicz A; Shear stress increases endothelial hyaluronan synthase 2 and hyaluronan synthesis especially in regard to an atheroprotective flow profile. *Exp Physiol. Date of publication: 6 May 2011.*

Impact factor: 3.2

Marki A, Ermilov E, Zakrzewicz A, Koller A, Secomb T W, Pries A R; **Tracking of fluorescence nanoparticles with nanometer resolution in a biological system: assessing local viscosity and microrheology.** *Biomech Model Mechanobiol, 2013 June 11 (e-pub date)*

Florian T, Vorderwülbecke B J, Marki A, Krueger K, Liu Y, Baumunk D, Zakrzewicz A, Tepel M; **Pulsatile atheroprone shear stress affects the expression of transient repecetor potential channels in human endothelial cells.** *Hypertension 2012;59:1232-1240.*

Vorderwülbecke B J, Maroski J, Fiedorowicz K, Silva-Azevedo L, Marki A, Pries A R, Zakrzewicz A; **Regulation of endothelal connexin40 expression by shear stress.** *Am J Physiol Heart Circ Physiol, 2012;302:H143-H152.*

Maroski J, Vorderwülbecke B J, Fiedorowicz K, Silva-Azevedo L, Siegel G, Marki A, Pries A R, Zakrzewicz A; **Shear stress increases endotheilal hyaluronan syntase 2 and hyaluronan synthesis especially in regard to an atheroprotective flow profile.** *Exp Physiol, 2011;96.9:977-986.*

Curriculum vitae

Mein Lebenslauf wird aus datenschutzrechtlichen Gründen in der elektronischen Version meiner Arbeit nicht veröffentlicht.

Acknowledgements

I would like to wholeheartedly thank the support and patients of my supervisors Andreas Zakrzewicz and Axel Pries,
colleagues,
friends and family.

Berlin, 21.1.2014

Alex Marki, MD